Int. J. Heat Mass Transfer. Vol. 14, pp. 653–666. Pergamon Press 1971. Printed in Great Britain

CARTESIAN GRAETZ PROBLEMS WITH AIR PROPERTY VARIATION

K. W. SCHADE*
Stanford University, California, U.S.A.
and
D. M. McELIGOT†
Imperial College of Science and Technology, London, England

(*Received* 20 *April* 1970 *and in revised form* 8 *June* 1970)

Abstract—Heat transfer and wall friction results have been obtained numerically to demonstrate the effects of gas transport property variation on three classical, laminar flow situations: (a) heating and cooling at constant wall temperature with a fully developed velocity profile at entry, (b) heating and cooling at constant wall temperature with a uniform velocity profile at entry, and (c) heating with constant wall heat flux and a uniform velocity profile at the entrance.

NOMENCLATURE

A_{cs}, cross sectional area;
b, exponent for conductivity in power law, equation (2b);
c_p, specific heat at constant pressure;
d, exponent for specific heat in power law, equation (2b);
D_h, hydraulic diameter (twice plate spacing);
g_c, dimensional constant, e.g. 32·17 [ft lbm/lbf-s^2];
G, average mass flux, $\dot{m}/A_{cs}$;
h, enthalpy;
k, thermal conductivity;
$\dot{m}$, mass flow rate;
p, pressure;
q''_w, wall heat flux;
T, absolute temperature;
u, axial velocity;
v, transverse velocity;
V_b, bulk velocity, G/ρ_b; V_0, entering bulk velocity;
x, axial coordinate;
y, transverse coordinate.

Dimensionless groups

f, local friction factor; f_{app}, based on one-dimensional, apparent wall shear stress defined in text; f_s, based on local wall velocity gradient, $\mu_w(\partial u/\partial y)_w/(G^2/2g_c\rho_b)$;
Nu, local Nusselt number, $q''_w D_h/k(T_w - T_b)$; Nu_∞, for fully developed flow;
P^+, pressure deficit, $(p_0 - p)/(G^2/2g_c\rho_0)$;
Pr, Prandtl number, $c_p\mu/k$;
Re, Reynolds number, GD_h/μ;
x^+, axial distance parameter, $4x/(D_h RePr)$.

Greek symbols

θ, normalized local bulk temperature, $(T_b - T_0)/(T_w - T_0)$;
μ, absolute viscosity;
ρ, density;
τ_w, wall shear stress.

Subscripts

b, properties evaluated at local bulk temperature;
cp, based on constant property idealizations;
0, entry conditions;
w, properties evaluated at wall temperature;
∞, asymptotic value.

* Formerly NDEA Fellow, Aerospace and Mechanical Engineering Department, The University of Arizona, Tucson, Ariz., U.S.A.
† On leave from the University of Arizona.

RECENT improvements in digital computers now permit the standard laminar heat-transfer problems to be calculated readily. However, with gas properties varying due to their temperature dependence, the solutions for strong heating or strong cooling are slightly more difficult because the governing partial differential equations become coupled. Bankston and McEligot and others [1–4] have presented methods for solving the resulting system of equations for internal, boundary-layer flow.

For the present paper, the method of Bankston and McEligot has been applied to three classical problems for heat transfer with forced convective flow between parallel plates and symmetrical boundary conditions. A fourth version—heating at a specified wall heat flux after an adiabatic entry provides fully developed flow—has recently been solved by Swearingen and McEligot with an alternate numerical approach [5]. In each case air properties are modeled by power laws.

The results are important for two reasons. Turbulent flow with property variation may now be tackled numerically. But it is necessary to ensure that computer programs for such problems yield correct results when the transport properties are not ambiguous—i.e. for laminar flow. Otherwise, programming errors in those terms which become significant only with property variation could yield behaviour which would be taken, mistakenly, as the effect of the turbulence model. The present tabulated results provide a means of testing such programs. Secondly, for applications in the process industries the ratio of "heat-transfer-power" to "pumping power" increases as the Reynolds number is decreased from the turbulent range to and through laminar flow. For gas flows, the fraction of the overall energy budget which is used for pumping the fluid can be appreciable. Hence, laminar flow heat exchangers currently are finding increasing favour [6] and, thus, results for laminar flow with property variation become useful, in their own right, for practical application.

APPROACH

Under the usual boundary layer approximations, plus the assumptions that (a) Mach number $\ll 1$, (b) $RePr \gtrsim 100$, and (c) natural convection is negligible, the governing differential equations become:

Continuity:

$$\frac{\partial}{\partial x}(\rho u) + \frac{\partial}{\partial y}(\rho v) = 0 \tag{1a}$$

X-momentum:

$$\rho u \frac{\partial u}{\partial x} + \rho v \frac{\partial u}{\partial y} = -g_c \frac{\mathrm{d}p}{\mathrm{d}x} + \frac{\partial}{\partial y}\left(\mu \frac{\partial u}{\partial y}\right) \tag{1b}$$

Energy:

$$\rho u \frac{\partial h}{\partial x} + \rho v \frac{\partial h}{\partial y} = \frac{\partial}{\partial y}\left(k \frac{\partial T}{\partial y}\right) \tag{1c}$$

Integral continuity*:

$$\rho_0 v_0 A_{cs} = \int_{A_{cs}} \rho u \, \mathrm{d}y. \tag{1d}$$

Initial conditions are (1) $T(y,0) = T_0$, and (2) $u(y,0)$ is either fully-developed or uniform. Boundary conditions are (1) the no-slip conditions for velocities and (2) either T_w specified or q''_w specified. The boundary conditions are symmetrical.

Gas properties are described by the equation-of-state for a perfect gas,

$$(\rho/\rho_0) = (pT_0)/(p_0 T) \tag{2a}$$

and by transport properties approximated for air,†

$$\frac{\mu}{\mu_0} = \left(\frac{T}{T_0}\right)^{0.67}, \quad \frac{k}{k_0} = \left(\frac{T}{T_0}\right)^{0.805}, \quad \frac{c_p}{c_{p,0}} = \left(\frac{T}{T_0}\right)^{0.095} \tag{2b}$$

* The integral continuity equation introduces the physical information that the transverse velocity is zero at the second wall, a second boundary condition which could not be used with equation (1a).

† The exponents have been estimated by graphically fitting the tabulations of properties in NBS 564 [9].

The essentials of the numerical method are described elsewhere [1] and will not be repeated here. It is a finite-control-volume analysis with implicit algebraic equations which are iterated to treat the non-linearities and coupling. A listing of the basic computer program for asymmetric thermal boundary conditions is available in a report by Schade [7].

The mesh spacing increases in both the transverse and axial directions. For the results reported here, 81 traverse nodes were employed with the first usually at $(y/D_h) = 0.001$, and longitudinally there were 20 steps per decade normally starting at $x_0^+ = 10^{-5}$.

As noted by Worsoe-Schmidt and Leppert [2], the boundary layer approximations are not appropriate for $x^+ < 10^{-3}$ so no results are reported for the initial two axial decades.* Tests at $(T_w/T_0) = 10$ showed convergence within 2 per cent for Nu and within $\frac{1}{2}$ per cent for f_s; this level of accuracy is considered adequate for practical purposes.

FULLY DEVELOPED ENTRY FLOW

Results are listed in terms of pertinent wall parameters in Table 1. There a number of the quantities are those normally presented from analyses; these are provided for comparison to treatments which may be developed for other geometries. The Nusselt numbers under the constant properties assumption, calculated by setting the exponents in equation (2b) to zero, agree with the predictions of McCuen *et al.* [8] to within 2 per cent of $x^+ = 0.004$ and otherwise within 1 per cent. Less familiar parameters are presented to aid engineers in the direct application of the present results; their use will be explained presently.

* Though an approach using a numerical program for systems of elliptic partial differential equations might be thought preferable in order to avoid the boundary layer approximations, for the problems studied excessive computer storage and time currently would be necessary to achieve the modest accuracy desired.

Heat transfer

Nusselt numbers, based on bulk properties, are plotted in Fig. 1 vs. the axial distance parameter, x_0^+, based on entering fluid properties. It is observed that there is a moderate increase at a specified axial location when heating and a moderate decrease when cooling the gas. Though not shown, all curves approach $Nu_\infty = 7.54$ downstream as T_w/T_b approaches unity. Worsoe-Schmidt and Leppert [2] found the same tendencies for a circular tube.

The appropriate application is the prediction of the bulk temperature of a gas which is being cooled or heated—or prediction of the distance necessary to reach a specified bulk temperature. If only Nusselt numbers are presented, the problem becomes iterative. Since the effect on the Nusselt number is moderate, one might be tempted to use the results of the available constant properties solution. Shown in Fig. (2a) are the unexpected results: with heating, thermal

Table 1. *Wall parameters for air flow. Fully-developed velocity profile at entry, constant wall temperature*

x_0^+	$\frac{T_b - T_0}{T_w - T_0}$	Nu_b	$\frac{T_w}{T_b}$	$\frac{f_{app} \cdot Re_b}{24}$	$\frac{f_s \cdot Re_b}{24}$	$\frac{p_0 - p}{G^2/(2g_c\rho_0)}$	$\frac{p_0 - p}{(p_0 - p)_{w,fd}}$
			$(T_w/T_0) = 10$				
0·001	0·0572	30·2	6·60	6·06	7·55	1·20	1·53
0·002	0·0908	22·1	5·50	5·69	6·07	2·04	1·30
0·005	0·169	14·6	3.97	4·72	4·21	4·40	1·12
0·01	0·274	11·0	2·89	3·80	3·05	8·51	1·08
0·02	0·445	9·00	2·00	2·47	2·04	17·4	1·10
0·05	0·782	7·90	1·24	1·25	1·20	42·7	1·09
0·1	0·961	7·59	1·04	1·03	1·03	82·5	1·05
0·2	0·998	7·54	1·00	1·00	1·00	161·	1·03

Table 1—continued

x_0^+	$\frac{T_b - T_0}{T_w - T_0}$	Nu_b	$\frac{T_w}{T_b}$	$\frac{f_{app} \cdot Re_b}{24}$	$\frac{f_s \cdot Re_b}{24}$	$\frac{p_0 - p}{G^2/(2g_c\rho_0)}$	$\frac{p_0 - p}{(p_0 - p)_{w,fd}}$
			$(T_w/T_0) = 5$				
0·001	0·0445	27·7	4·25	5·74	4·42	0·520	2·10
0·002	0·0704	21·4	3·90	4·81	3·99	0·851	1·72
0·005	0·130	15·1	3·29	3·82	3·28	1·70	1·38
0·01	0·208	11·7	2·73	3·17	2·70	3·01	1·22
0·02	0·334	9·51	2·14	2·49	2·11	5·63	1·14
0·05	0·614	8·18	1·45	1·49	1·38	13·5	1·10
0·1	0·862	7·72	1·12	1·11	1·09	26·2	1·06
0·2	0·980	7·57	1·02	1·02	1·01	51·0	1·03
			$(T_w/T_0) = 2$				
0·001	0·0337	22·8	1·94	3·00	1·82	0·140	2·62
0·002	0·0534	18·2	1·90	2·54	1·78	0·229	2·14
0·005	0·0977	13·7	1·82	2·09	1·69	0·446	1·67
0·01	0·155	11·0	1·73	1·85	1·61	0·761	1·42
0·02	0·245	9·29	1·61	1·64	1·50	1·33	1·25
0·05	0·448	8·14	1·38	1·37	1·30	2·98	1·11
0·1	0·678	7·82	1·19	1·18	1·14	5·68	1·06
0·2	0·887	7·62	1·06	1·05	1·04	11·1	1·03
			$(T_w/T_0) = 1$, constant properties				
0·001	0·0288	19·9		1·00	1·00	0·0168	1·00
0·002	0·0456	16·0				0·0336	
0·005	0·0834	12·1				0·0841	
0·01	0·132	10·0				0·168	
0·02	0·207	8·57				0·336	
0·05	0·374	7·66				0·841	
0·1	0·569	7·55				1·68	
0·2	0·785	7·54				3·36	
0·5	0·973	7·54				8·41	
			$(T_w/T_0) = 0·5$				
0·001	0·0258	17·9	0·507	−0·340	0·655	−0·0440	−8·33
0·002	0·0408	14·5	0·510	−0·026	0·663	−0·0615	−5·83
0·005	0·0747	11·0	0·519	0·280	0·677	−0·0876	−3·32
0·01	0·118	9·17	0·531	0·445	0·692	−0·102	−1·92
0·02	0·184	7·90	0·551	0·596	0·716	−0·0904	−0·856
0·05	0·330	7·08	0·599	0·711	0·756	0·0284	0·107
0·1	0·500	7·04	0·667	0·775	0·800	0·282	0·534
0·2	0·701	7·20	0·770	0·835	0·858	0·812	0·769
0·5	0·927	7·44	0·932	0·948	0·956	2·41	0·912
			$(T_w/T_0) = 0·2$				
0·001	0·0232	16·7	0·204	−1·26	0·484	−0·0784	−68·6
0·002	0·0372	13·4	0·206	−0·740	0·495	−0·116	−50·8
0·005	0·0685	10·2	0·212	−0·207	0·513	−0·186	−32·6
0·01	0·108	8·50	0·219	0·071	0·530	−0·253	−22·1
0·02	0·169	7·33	0·231	0·298	0·554	−0·323	−14·1
0·05	0·301	6·54	0·264	0·520	0·599	−0·382	−6·68
0·1	0·454	6·46	0·314	0·602	0·635	−0·365	−3·19
0·2	0·635	6·62	0·407	0·645	0·680	−0·266	−1·16
0·5	0·863	7·01	0·646	0·769	0·794	0·0819	0·143
1·0	0·964	7·36	0·874	0·910	0·921	0·669	0·585

Table 1—continued

x_0^+	$\frac{T_b - T_0}{T_w - T_0}$	Nu_b	$\frac{T_w}{T_b}$	$\frac{f_{app} \cdot Re_b}{24}$	$\frac{f_s \cdot Re_b}{24}$	$\frac{p_0 - p}{G^2/(2g_c\rho_0)}$	$\frac{p_0 - p}{(p_0 - p)_{w,fd}}$
			$(T_w/T_0) = 0{\cdot}1$				
0·001	0·0224	16·2	0·102	−1·60	0·410	−0·0898	−250
0·002	0·0359	13·0	0·103	−0·988	0·427	−0·134	−187
0·005	0·0662	9·90	0·106	−0·400	0·451	−0·218	−121
0·01	0·105	8·24	0·110	−0·056	0·472	−0·302	−84·0
0·02	0·163	7·10	0·117	0·197	0·498	−0·396	−55·1
0·05	0·291	6·31	0·135	0·454	0·544	−0·505	−28·1
0·1	0·437	6·20	0·165	0·544	0·577	−0·548	−15·3
0·2	0·610	6·30	0·222	0·572	0·607	−0·549	−7·64
0·5	0·831	6·60	0·397	0·651	0·679	−0·459	−2·56
1·0	0·939	7·02	0·647	0·789	0·799	−0·269	−0·749

development is more rapid than anticipated from a casual glance at the Nusselt number curves. The higher wall temperature increases the thermal conductivity in the wall region, thus lowering the thermal resistance where it is most important. The lowered wall resistance leads to more rapid heating of the flow in the central region so the thermal resistance is reduced there, too, and the cumulative effect is a greater increase in the bulk temperature. Further, the reduced density accelerates the flow so that velocities are higher, also serving to reduce the thermal resistance; however, this effect would be expected to be reduced somewhat by the increased viscosity at the wall.

The above comparison is presented in terms of properties evaluated at the inlet bulk temperature, a quantity which one expects to be specified in a design application. However, one might argue that since the thermal resistance near the wall tends to be most important, properties should be evaluated at the wall temperature instead. Figure 2(b) demonstrates such a prediction. The thermal development for heating is not as rapid as if the properties are at the wall values throughout the field. While the difference from the constant properties prediction is reduced for strong heating it is magnified for cooling. Use of a film reference temperature in the presentation would likely collapse the

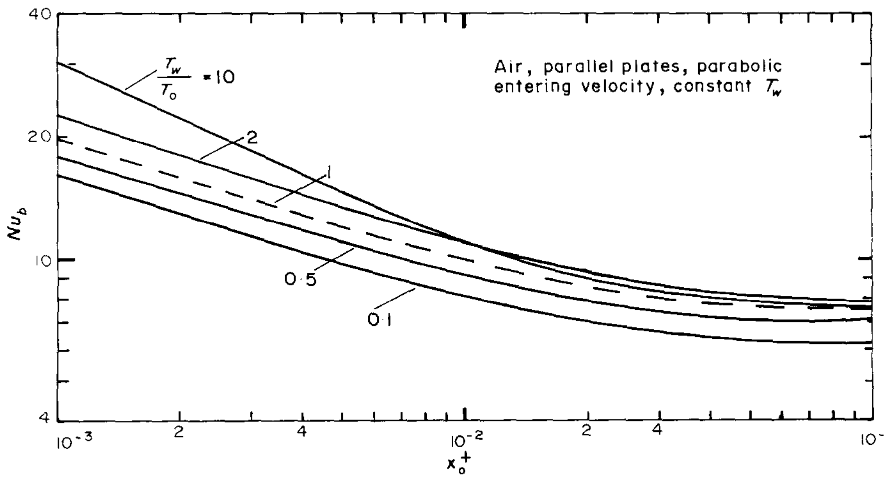

FIG. 1. Effect of air property variation on heat transfer for fully developed flow at entry.

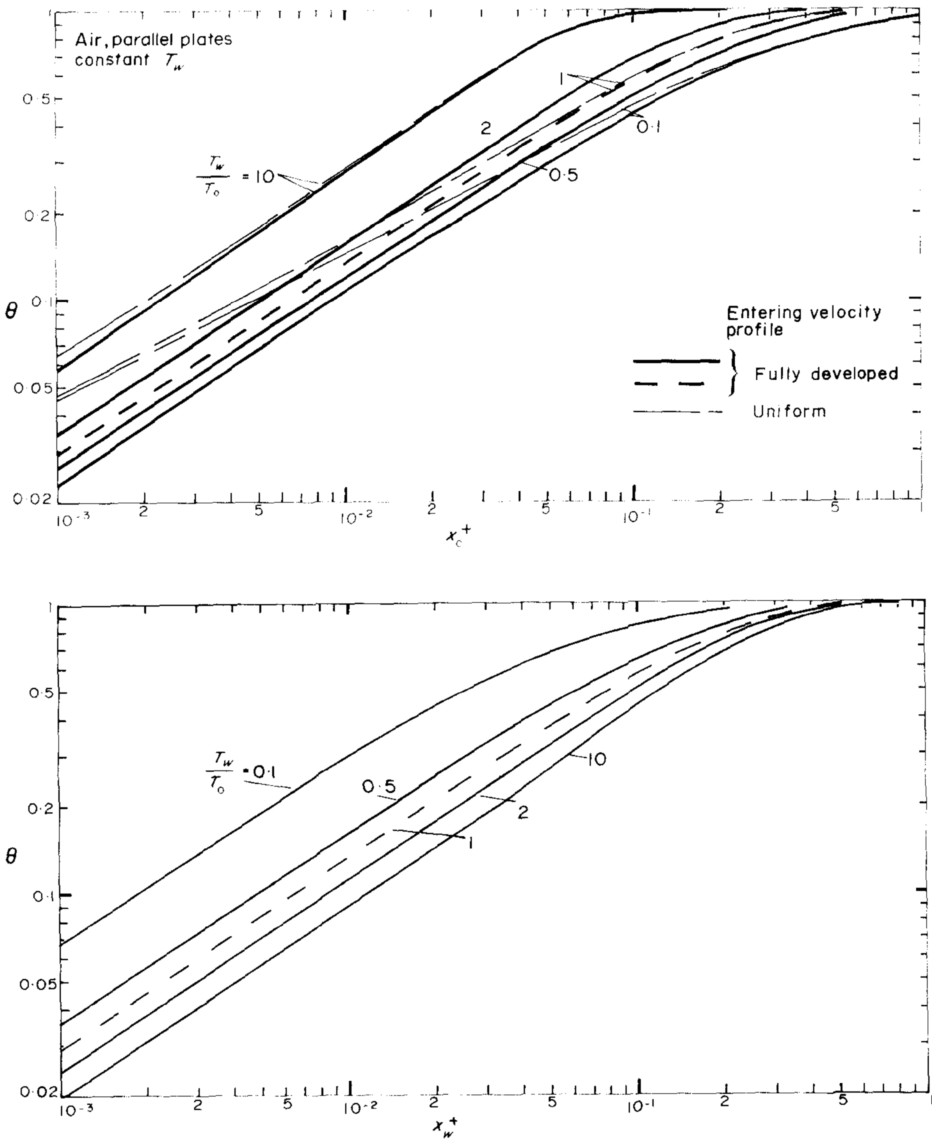

FIG. 2. Effect of air property on thermal development. (a) Comparison based on inlet properties. (b) Comparison based on wall properties.

curves towards the constant property prediction but the design problem would again become iterative.

For applications where the objective is to bring the temperature of a gas stream to the value at the wall, the following correlation approximates the downstream thermal development:

$$\theta = \frac{T_b - T_0}{T_w - T_0} \cong 1 - 0{\cdot}85\,[0{\cdot}33 \ln (T_w/T_0) - 0{\cdot}03\,(T_w/T_0) + 1{\cdot}03] \exp(-7x_w^+). \quad (3)$$

For $x_w^+ \gtrsim 0{\cdot}15$ this correlation described the numerical results within about 2 per cent. Thus, for heating the relation describes the last 30–40 per cent of thermal development but may only treat the last ten per cent for severe cooling.

The comparison of Figs. (2a) and (2b) demonstrates the importance of property variation and indicates the difficulty in application of results based on assumption of constant properties. For cooling there is another subtle effect of the temperature dependence typical of gases. One normally expects that a fluid will be cooled to a desired temperature in a significantly shorter distance if the wall temperature is decreased considerably. With strong cooling one may be somewhat disappointed. If we transpose the results to a more direct indication,

$$\frac{T_b}{T_0} = \left(\frac{T_b - T_0}{T_w - T_0}\right)\left(\frac{T_w}{T_0} - 1\right) + 1$$

we find that the local bulk temperature in the thermal entrance region is reduced almost as rapidly when $(T_w/T_0) = \frac{1}{5}$ as when $(T_w/T_0) = \frac{1}{10}$. For example, even at $x_0^+ = 0{\cdot}1$, (T_b/T_0) equals 0·64 for $(T_w/T_0) = \frac{1}{5}$ but is only slightly lower (0·61) when the imposed cooling is at $(T_w/T_0) = \frac{1}{10}$. It is believed that the cause is offsetting of larger temperature difference by the reduced wall conductivity. So in some practical problems an attempt to use lower wall temperatures may not be worth the effort.

Pressure distribution

The design parameter for wall friction is the apparent friction factor, f_{app}, based on the one-dimensional apparent wall shear stress,

$$\tau_{w,\,\text{app}} = -\frac{D_h}{4}\frac{\mathrm{d}}{\mathrm{d}x}\left\{p + \frac{G^2}{\rho_b g_c}\right\}.$$

This quantity will differ significantly from the friction factor based on the velocity gradient at

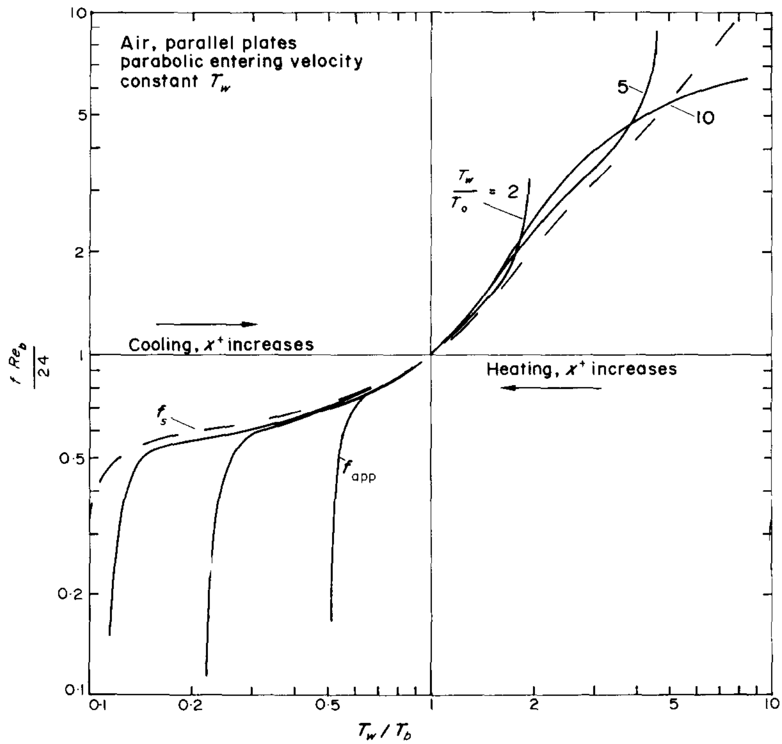

FIG. 3. Effect of air property variation on wall friction for fully developed flow at entry.

the wall, f_s, where the velocity profile is undergoing major readjustment due to strong heat transfer.

The variation of f_{app} is shown in Fig. 3 for several tabulated conditions. In each case the parameters approach unity as x^+ increases. One sees that the curves approximately approach a single function, $f_{app} \cdot Re_b\{T_w/T_b\}$, after the initial readjustment region. For the present results, the function may be approximated as:

$$f_{app} \cdot Re_b \cong 24(T_w/T_b)^{1.2} \text{ for heating} \tag{4a}$$

and

$$f_{app} \cdot Re_b \cong 24 \exp(-0.73[1 - (T_w/T_b)]) \text{ for cooling} \tag{4b}$$

for $z_w^+ \gtrsim 0.03$*. As shown by the dashed lines ($T_w/T_0 = 10$ and $\frac{1}{10}$) the behavior of $f_s \cdot Re_b$ is comparable in the same region. The magnitudes differ slightly but the main difference is that f_s behaves more smoothly in the readjustment region for $x_w^+ \lesssim 0.03$. Unfortunately, f_s is of no use in one-dimensional design calculations.

The axial pressure distribution may be presented directly in terms of P^+, the pressure deficit. Typically, this quantity is defined in terms of the known entering properties,

$$P^+ = \frac{p_0 - p}{G^2/2g_c\rho_0}.$$

In this form P^+ is listed in Table 1 to show the effects of the fluid property variation. Again there are unexpected results. For cooling conditions the pressure is found to rise in the thermal entrance.†

One may investigate the plausibility of a rising pressure by considering the problem in two parts—the effect of deceleration and the effect of the reduced wall viscosity. The momentum component of the axial pressure change from the fully developed profile at T_0 to the fully developed profile at T_w is:

$$\frac{(p_0 - p_\infty)_{mom}}{G^2/2g_c\rho_0} \cong \frac{12}{5}\left(\frac{T_w}{T_0} - 1\right).$$

The major part of this change will occur by $x_w^+ \approx 0.2$ or so. For order-of-magnitude comparison, we calculate the distance necessary to develop the same change in pressure if there were only viscous effects and the flow were fully developed at T_w throughout. The pressure drop for fully developed flow is:

$$\frac{(p_0 - p_x)_{fd}}{G^2/2g_c\rho_0} \approx 24Pr_w x_w^+(T_w/T_0)$$

$$\cong 24Pr_0 x_0^+(T_w/T_0)^{1+0.67}.$$

At $(T_w/T_0) = \frac{1}{10}$, we see that the distance required would be $x_0^+ \approx 6.5$ while the overall momentum change occurs by $x_0^+ = 0.5$–1. So the pressure rise is plausible and the numerical predictions show that it would occur, somewhat to the surprise of the reader accustomed to solutions of the Graetz problem based on constant properties.

As noted earlier, it is sometimes useful to consider the application in terms of properties evaluated at the wall temperature. The final column of the table then provides a means of estimating the resulting error in the predicted pressure drop if it is considered as fully developed at T_w throughout. The prediction would be

$$p_{w,fd}^+ = \frac{(p_0 - p_x)}{G^2/2g_c\rho_w} = 24Pr_w x_w^+$$

and the table presents $(p_0 - p_x)/(p_0 - p_x)_{w,fd}$, the correction factor to apply in order to obtain the same value as the present numerical predictions. For moderate heating the correction becomes small at practical distances. Eventually, the correction factor will approach unity in all cases.

* The axial distance parameter based on wall properties is given by

$$x_w^+ = \frac{4x}{D_h Re_w Pr_w} = x_0^+\left(\frac{T_w}{T_0}\right)^{b-d}.$$

† R. W. Shumway, of The University of Arizona, found this effect earlier in unpublished calculations for flow in a circular tube with $T_w/T_0 \approx 1.25$.

UNIFORM ENTRY FLOW

Constant wall temperature

The simultaneous entry problem with a step change to a high wall temperature was the most difficult of the three general problems studied. Since the difficulty emphasizes the inadequacy of the boundary-layer equations for very short distances, it will be discussed briefly.

In the finite difference representation, the velocity near the wall is decelerated from the uniform entering value to a value near zero within the distance specified as the first step. In the same distance the wall temperature is increased abruptly so the fluid density drops severely near the wall. Consequently, most of the mass entering the finite control volume for the node adjacent to the wall could be required to leave in the transverse direction rather than the axial direction. For example, at $(T_w/T_0) = 10$ and with a fine grid, the transverse flow rate is about 96 per cent of the entering flow rate for this control volume.

In addition to violating the boundary layer approximations, the large transverse flow can lead to a divergent sequence in the iterative process at the first step. On successive iterations more and more energy would be carried by transverse convection, causing the calculated thermal boundary layer to extend further towards the centerplane and, in turn, lowering the local density, further from the wall and increasing transverse velocities to continue the process. Eventually the calculations can lead to large negative axial velocities near the wall and to the possibility of an isothermal temperature across the channel as a limiting result. In the present study, such a divergent process occurred for $(T_w/T_0) > 5$. Even the normally reliable tactic of weighted successive substitution of the variables (or "under-relaxation") failed to avoid it. Presumably, the same difficulty would arise in the case with the fully developed entering flow if the step in wall temperature were sufficiently large. With strong heating at a specified heat flux this difficulty does not occur because wall temperatures are low at small x^+.

For this case—constant wall temperature and uniform entering velocity—the calculations were started at $x_0^+ = 10^{-6}$. The node adjacent to the wall was at $(y/D_h) = 0{\cdot}0002$. Iteration converged at the first step for $(T_w/T_0) < 2$. For $(T_w(T_0) = 5$ and 10, the wall temperature was increased successively up to the specified value within the first twenty steps. Thus, the thermal boundary condition was equivalent to a finite difference "step" by $x_0^+ = 10^{-5}$, the initial step for the other two cases investigated. Before $x_0^+ = 10^{-3}$ the transverse velocities are sufficiently small for the internal boundary-layer approximations to be valid. Table 2 lists results.

In the constant properties runs, it was found that several iterations were necessary at each step in the developing region in order to obtain convergence of the velocity profile. Otherwise, the resulting energy balance could be significantly in error. This observation should serve as a caution that numerical methods which attempt to reduce computer time by avoiding iteration in boundary layer problems must carefully test convergence with respect to the size of longitudinal steps.

The flow development effects either augment the effects of the gas property variation or oppose them, depending on whether the gas is being heated or cooled. For *heat transfer*, the results with and without a simultaneous flow entry approach each other as the fully developed condition is approached (for specified T_w/T_0). Comparison for the two extreme cases and for constant properties is added to Fig. 2a. One sees the entry effects of flow development caused by heating and flow development after a uniform entry are in the same direction—the heat transfer to the bulk fluid increases. Consequently, the two augment each other. However, at high wall temperatures such as $(T_w/T_0) = 10$ the heating effects dominate so that, beyond $x_0^+ \cong 0{\cdot}002$, θ and Nu_b are approximately the same for both flow entry conditions. As the wall temperature is reduced, the flow entry becomes more dominant at low x_0^+ and its effects persist further downstream. Thus, at $(T_w/T_0) = 0{\cdot}1$, the

Table 2. Wall parameters for air flow. Uniform velocity profile at entry, constant wall temperature

x_0^+	$\dfrac{T_b - T_0}{T_w - T_0}$	Nu_b	$\dfrac{T_w}{T_b}$	$\dfrac{f_{app} \cdot Re_b}{24}$	$\dfrac{f_s \cdot Re_b}{24}$	$\dfrac{p_0 - p}{G^2/(2g_c\rho_0)}$	$\dfrac{p_0 - p}{(p_0 - p)_{w,fd}}$
			$(T_w/T_0) = 10$				
0·001	0·0645	30·6	6·33	8·26	8·12	1·61	2·05
0·002	0·0990	22·0	5·29	6·64	6·25	2·54	1·61
0·005	0·178	14·4	3·85	4·94	4·21	5·06	1·29
0·01	0·282	10·9	2·83	3·81	3·02	9·29	1·18
0·02	0·452	8·96	1·97	2·43	2·01	18·2	1·16
0·05	0·785	7·89	1·20	1·24	1·19	43·6	1·11
0·1	0·962	7·59	1·04	1·03	1·03	83·5	1·06
0·2	0·998	7·54	1·00	1·00	1·00	162·	1·03
			$(T_w/T_0) = 5$				
0·001	0·0550	29·4	4·10	9·05	5·61	0·835	3·38
0·002	0·0824	21·9	3·76	6·55	4·61	1·25	2·52
0·005	0·143	15·0	3·18	4·44	3·48	2·22	1·80
0·01	0·221	11·6	2·66	3·39	2·75	3·65	1·48
0·02	0·346	9·44	2·10	2·52	2·10	6·37	1·29
0·05	0·622	8·16	1·43	1·48	1·37	14·3	1·16
0·1	0·865	7·71	1·12	1·11	1·09	27·0	1·09
0·2	0·980	7·57	1·02	1·02	1·01	51·9	1·05
0·5	1·00	7·54	1·00	1·00	1·00	126	1·02
			$(T_w/T_0) = 2$				
0·001	0·0485	26·7	1·91	7·18	3·49	0·354	6·63
0·002	0·0708	20·2	1·87	5·12	2·83	0·509	4·76
0·005	0·118	14·2	1·79	3·36	2·21	0·840	3·14
0·01	0·176	11·2	1·70	2·49	1·87	1·26	2·35
0·02	0·265	9·27	1·58	1·90	1·59	1·94	1·81
0·05	0·464	8·11	1·37	1·40	1·30	3·68	1·38
0·1	0·687	7·81	1·19	1·17	1·14	6·41	1·20
0·2	0·890	7·62	1·06	1·05	1·04	11·8	1·10
0·5	0·996	7·55	1·00	1·00	1·00	27·9	1·04
			$(T_w/T_0) = 1$, constant properties				
0·001	0·0465	25·7		5·40	2·85	0·180	10·7
0·002	0·0669	19·2		3·87	2·22	0·255	7·59
0·005	0·109	13·4		2·55	1·66	0·409	4·87
0·01	0·159	10·5		1·89	1·37	0·591	
0·02	0·234	8·72		1·45	1·28	0·863	2·57
0·05	0·396	7·65		1·10	1·04	1·48	1·76
0·1	0·584	7·54		1·01	1·00	2·35	1·40
0·2	0·793	7·54		1·00	1·00	4·04	1·20
0·5	0·974	7·54		1·00	1·00	9·08	1·08
			$(T_w/T_0) = 0·5$				
0·001	0·0457	25·2	0·512	4·12	2·63	0·0864	16·4
0·002	0·0651	18·6	0·517	2·98	1·98	0·122	11·6
0·005	0·105	12·8	0·528	1·98	1·41	0·193	7·32
0·01	0·151	10·0	0·541	1·48	1·13	0·274	5·19
0·02	0·218	8·22	0·561	1·14	0·945	0·389	3·68
0·05	0·358	7·12	0·609	0·872	0·821	0·625	2·37
0·1	0·520	7·05	0·676	0·806	0·814	0·919	1·74
0·2	0·712	7·21	0·776	0·841	0·863	1·46	1·38
0·5	0·929	7·45	0·934	0·950	0·958	3·05	1·16
0·95	0·990	7·53	0·991	0·994	0·995	5·43	1·08

Table 2—continued

x_0^+	$\frac{T_b - T_0}{T_w - T_0}$	Nu_b	$\frac{T_w}{T_b}$	$\frac{f_{app} \cdot Re_b}{24}$	$\frac{f_s \cdot Re_b}{24}$	$\frac{p_0 - p}{G^2/(2g_c\rho_0)}$	$\frac{p_0 - p}{(p_0 - p)_{w, fd}}$
			$(T_w/T_0) = 0{\cdot}2$				
0·001	0·0452	24·9	0·208	3·20	2·57	0·0278	24·3
0·002	0·0642	18·3	0·211	2·33	1·90	0·0392	17·2
0·005	0·102	12·5	0·218	1·56	1·30	0·0618	10·8
0·01	0·146	9·64	0·226	1·18	1·00	0·0868	7·59
0·02	0·208	7·81	0·240	0·927	0·815	0·121	5·30
0·05	0·334	6·62	0·273	0·722	0·679	0·185	3·24
0·1	0·477	6·48	0·324	0·649	0·655	0·248	2·17
0·2	0·649	6·64	0·416	0·654	0·686	0·357	1·56
0·5	0·867	7·02	0·653	0·773	0·798	0·707	1·24
0·95	0·955	7·34	0·862	0·902	0·915	1·23	1·14
			$(T_w/T_0) = 0{\cdot}1$				
0·001	0·0450	24·7	0·104	2·86	2·53	0·00782	21·8
0·002	0·0638	18·2	0·106	2·09	1·87	0·0112	15·6
0·005	0·101	12·3	0·110	1·41	1·27	0·0178	9·93
0·01	0·144	9·49	0·115	1·07	0·975	0·0251	7·00
0·02	0·204	7·65	0·122	0·851	0·779	0·0350	4·87
0·05	0·326	6·41	0·142	0·671	0·635	0·0511	2·84
0·1	0·462	6·22	0·171	0·596	0·601	0·0567	1·58
0·2	0·625	6·31	0·229	0·581	0·613	0·0684	0·952
0·5	0·836	6·62	0·404	0·654	0·682	0·162	0·900
0·95	0·935	6·99	0·631	0·766	0·789	0·332	0·972

two curves for θ do not begin to coincide until $x_0^+ \approx 0{\cdot}2$. Since the downstream behavior is approximately the same for both entry conditions, equation (3) should again be a useful correlation.

The *wall friction* and pressure drop parameters show the same trends as for heat transfer, but the behavior imposed by the uniform entry persists further downstream. The most obvious change is that for the strongly cooled runs the flow development from the uniform entering velocity counteracts the thermal readjustment and there is no longer a pressure rise. At $(T_w/T_0) = 0{\cdot}1$, however, the pressure drop is almost nil in the entry region. At the other extreme, $(T_w/T_0) = 10$, the pressure deficit becomes almost independent of the entering velocity profile around $x_0^+ \approx 0{\cdot}02$ (instead of 0·002 as for heat transfer).

For heating, a design approximation using the fully developed flow prediction based on wall properties would yield pressure drops within ten per cent by $x_0^+ = 0{\cdot}5$. However, for some cooling situations one would have to go beyond $x_0^+ = 1$ for the same level of approximation.

In passing, it is perhaps appropriate to comment on the equivalent turbulent flow problem. The authors have examined *cooling* of a turbulent stream of air with a short flow development section and have found good agreement with data for rectangular duct flow to $(T_w/T_0) \cong \frac{1}{3}$ [10]. The wall temperature was kept roughly constant. In contrast to the laminar case, the downstream predictions show an increase in both Nusselt number and friction factor when compared to results based on constant property idealisations. And, rather than differing significantly in trend, both Nu/Nu_{cp} and f/f_{cp} increase approximately as the $-\frac{1}{3}$ power of the local T_w/T_b.

Constant wall heat flux

Under the constant properties idealization the flow development is independent of thermal boundary conditions. Accordingly, comparison of the constant properties runs in Table 2 and in Table 3 demonstrates the combined effect of the initial step size and the transverse node spacing near the wall. The few third digit differences between the friction parameters are acceptable.

With specified q''_w, the bulk temperature may be determined directly at any axial location by an energy balance. As a consequence, the Nusselt number is a more useful result than it

Table 3. Wall parameters for air flow. Uniform velocity profile at entry, constant wall heat flux

x_0^+	T_b/T_0	T_w/T_b	Nu_b	$\dfrac{f_{app} \cdot Re_b}{24}$	$\dfrac{f_x \cdot Re_b}{24}$	$\dfrac{p_0 - p}{G^2/(2g_c\rho_0)}$
			$[q''_w D_h/(k_0 T_0)] = 0$, constant properties			
0·001			34·5	5·38	2·84	0·177
0·002			25·4	3·87	2·22	0·252
0·005			17·4	2·55	1·65	0·406
0·01			13·4	1·89	1·37	0·587
0·02			10·7	1·44	1·18	0·860
0·05			8·73	1·10	1·04	1·48
0·1			8·29	1·01	1·00	2·35
0·2			8·24	1·00	1·00	4·03
			$[q''_w D_h/(k_0 T_0)] = 50$			
0·001	1·05	2·26	36·3	8·83	3·87	0·363
0·002	1·10	2·54	27·3	6·53	3·49	0·603
0·005	1·25	2·78	18·9	4·49	3·13	1·24
0·01	1·49	2·70	14·3	3·51	2·79	2·28
0·02	1·97	2·34	11·1	2·79	2·31	4·53
0·05	3·33	1·64	8·96	1·76	1·56	12·8
0·1	5·51	1·27	8·54	1·33	1·21	31·9
0·2	9·64	1·10	8·35	1·19	1·08	104
			$[q''_w D_h/(k_0 T_0)] = 100$			
0·001	1·10	3·25	37·5	9·90	4·84	0·515
0·002	1·20	3·56	28·2	7·11	4·50	0·886
0·005	1·49	3·57	19·0	4·84	3·91	1·94
0·01	1·97	3·12	13·9	3·87	3·24	3·77
0·02	2·89	2·40	10·6	2·97	2·43	8·10
0·05	5·51	1·52	8·80	1·62	1·45	24·8
0·1	9·64	1·20	8·46	1·26	1·15	66·8
0·2	17·5	1·07	8·31	1·17	1·05	246
			$[q''_w D_h/(k_0 T_0)] = 200$			
0·001	1·20	4·70	39·0	9·91	6·44	0·771
0·002	1·39	4·83	28·7	6·97	5·86	1·37
0·005	1·97	4·22	18·4	5·02	4·60	3·19
0·01	2·89	3·26	13·1	4·13	3·44	6·69
0·02	4·65	2·25	9·96	2·88	2·32	15·6
0·05	9·64	1·39	8·66	1·45	1·32	50·5
0·1	17·5	1·14	8·40	1·21	1·11	149
0·2	32·2	1·05	8·29	1·15	1·04	618

is with specified T_w. From Table 3, however, one may see that the effects of property variation follow the trends discussed earlier for constant T_w, only the magnitudes differ slightly. The differences do not warrant detailed discussion so the results will be summarized briefly.

Heat transfer and wall friction parameters increase as the heating rate increases, but in the entry region the improvement in Nu is only slightly greater than the effect caused by flow development alone. Wall friction is affected to a larger extent than Nu. Fully developed values are approached more rapidly as heating increases, but well downstream parameters still exceed those for constant properties.

Results again differ from the equivalent turbulent problem. Downstream, turbulent predictions and data for heating gases in circular tubes show a greater effect on heat transfer than on wall friction [11]. The variation of f is not as severe as for laminar flow but it is in the opposite direction; f_s/f_{cp} drops at about the $-0{\cdot}2$ to $-0{\cdot}3$ power of the local T_w/T_b. Nu/Nu_{cp} meanwhile varies approximately as the $-0{\cdot}4$ to $-0{\cdot}7$ power for significant heating at a specified wall heat flux.

CONCLUSIONS

The effects of gas property variation on the laminar flow of air between parallel plates are slight to moderate for heat transfer and more severe for wall friction and axial pressure distribution. For all cases studied, transport parameters increase with heating and deteriorate under cooling in comparison to constant property behavior. To engineers accustomed to working with constant property analyses, the results can be surprising and they show that the constant property idealization may lead to either dangerous or conservative design, depending on the application.

ACKNOWLEDGEMENTS

The work reported has been partially supported by the U.S. Army Research Office, Durham, and by the U.S. Army Mobility Equipment Research and Development Center, Fort Belvoir. The aid of the Computer Centers at The University of Arizona and the University of London is appreciated.

REFERENCES

1. C. A. Bankston and D. M. McEligot, Turbulent and laminar heat transfer to gases with varying properties in the entry region of circular ducts, *Int. J. Heat Mass Transfer* **13**, 319–344 (1970).
2. P. M. Worsøe-Schmidt and G. Leppert, Heat transfer and friction for laminar flow of a gas in a circular tube at high heating rate, *Int. J. Heat Mass Transfer* **8**, 1281–1301 (1965).
3. S. V. Patankar and D. B. Spalding, A finite difference procedure for solving the equations of the two-dimensional boundary layer, *Int. J. Heat Mass Transfer* **10**, 1389–1411 (1967).
4. R. G. Deissler and A. F. Presler, Analysis for developing laminar flow and heat transfer in a tube for a gas with variable properties, *Proc. Third Int. Heat Transfer Conf.*, **1**, 250–256 (1966).
5. T. B. Swearingen and D. M. McEligot, Internal laminar heat transfer with gas property variation, *J. Heat Transfer* in press.
6. W. M. Kays, Trends in heat exchanger design, First Annual Aerospace Heat Transfer Lecture, The University of Arizona (May 1965).
7. K. W. Schade, A numerical solution for the turbulent flow of a gas with strong property variation between parallel plates, M.S.E. Report, Aerospace and Mech. Eng. Dept., The University of Arizona (1969).
8. P. A. McCuen, W. M. Kays and W. C. Reynolds, Heat transfer with laminar and turbulent flow between parallel plates with constant and variable wall temperature and heat flux, Report AHT-3, Mech. Eng. Dept., Stanford University (1963).
9. J. Hilsenrath *et al.*, Tables of thermal properties of gases, NBS Circular 564 (1955).
10. K. W. Schade and D. M. McEligot, Turbulent flow between parallel plates with gas property variation, in preparation.
11. D. M. McEligot, S. B. Smith and C. A. Bankston, Quasi-developed turbulent pipe flow with heat transfer, *J. Heat Transfer* **92**, 641–650 (1970).

PROBLÈMES CARTÉSIENS DE GRAETZ AVEC VARIATION DES PROPRIÉTÉS DE L'AIR

Résumé—Des résultats de transfert thermique et de frottement pariétal sont obtenus numériquement afin de démontrer les effets de la variation des propriétés de transport d'un gaz dans trois situations classiques d'un écoulement laminaire: (a) Echauffement et refroidissement pour une température de paroi constante et un profil de vitesse entièrement développé à l'entrée. (b) Echauffement et refroidissement pour une température de paroi constante et un profil de vitesse uniforme à l'entrée. (c) Echauffement avec un flux de chaleur constant à la paroi et un profil de vitesse uniforme à l'entrée.

KARTESISCHES GRAETZ-PROBLEM MIT ÄNDERUNG DER LUFTEIGENSCHAFTEN

Zusammenfassung—Es wurden numerisch Ergebnisse für den Wärmeübergang und die Wandreibung ermittelt, um die Auswirkung veränderlicher Transporteigenschaften des Gases auf drei klassische Probleme laminarer Strömung zu zeigen:

(a) Beheizung und Kühlung bei konstanter Wandtemperatur mit hydrodynamisch voll ausgebildetem Geschwindigkeitsprofil am Eintritt;
(b) Beheizung und Kühlung bei konstanter Wandtemperatur mit gleichförmiger Geschwindigkeit am Eintritt, und
(c) Beheizung mit konstanter Wärmestromdichte und gleichfömiger Geschwindigkeit am Eintritt.

ЗАДАЧИ ГРЕТЦА В ДЕКАРТОВЫХ КООРДИНАТАХ ПРИ ПЕРЕМЕННЫХ СВОЙСТВАХ ВОЗДУХА

Аннотация—Приводятся результаты численных расчетов теплообмена и поверхностного трения на стенке, которые выявили влияние изменения свойств переноса газа в трех классических случаях ламинарного течения, а именно: (а) нагрев и охлаждение при постоянной температуре стенки при полностью развитом профиле скорости на входе, (б) нагрев и охлаждение при постоянной температуре стенки при однородном профиле скорости на входе, (в) нагрев при постоянном тепловом потоке на стенке и однородном профиле скорости на входе.